Single atoms coupled to a near-concentric cavity

Chi Huan Nguyen,[1] Adrian Nugraha Utama,[1] Nick Lewty,[1] Kadir Durak,[1] Gleb Maslennikov,[1] Stanislav Straupe,[1,2] Matthias Steiner,[1,3] and Christian Kurtsiefer[1,3]

[1]Centre for Quantum Technologies, 3 Science Drive 2, Singapore 117543
[2]Faculty of Physics, M.V. Lomonosov Moscow State University, Moscow, Russia
[3]Department of Physics, National University of Singapore, 2 Science Drive 3, Singapore 117542
(Dated: August 24, 2017)

Concentric cavities can lead to strong photon-atom coupling without a need for high finesse or small physical-cavity volume. In this proof-of-principle experiment we demonstrate coupling of single Rb atoms to a 11 mm long near-concentric cavity with a finesse $F = 138(2)$. Operating the cavity $1.7(1)\,\mu$m shorter than the critical length, we observe an atom-cavity coupling constant $g_0 = 2\pi \times 5.0(2)$ MHz which exceeds the natural dipole decay rate γ by a factor $g_0/\gamma = 1.7(1)$.

Introduction. Optical cavities are widely used in a range of modern instruments (e.g. lasers and optical clocks) and are essential for mediating interaction of light with other physical systems in many quantum technologies. In particular, by coupling atoms (or other quantum emitters) resonantly to a cavity, strongly interacting hybrid systems of light and matter can be realized [1]. This enhanced light-matter interaction is applied in quantum networks [2, 3] and quantum metrology [4, 5].

In cavity quantum electrodynamics (cavity QED) the conventional wisdom to realize a strongly coupled atom-cavity system employs short cavities with high finesse. The small mode volume V of these cavities results in a large coupling $g_0 \propto 1/\sqrt{V}$ between a single atom and a single cavity photon. In this situation g_0 exceeds the cavity field decay rate κ and the dipole decay rate of the atom γ, and the light-atom interaction is dominated by the coupling to the cavity mode. Unfortunately, these systems are experimentally demanding due to the need of ultra-high-reflectivity coatings and sophisticated techniques to trap single atoms in these short cavities. However, the notion that short cavities with high finesse are inevitable has been challenged by efforts to use a particular cavity geometry, a (near-)concentric cavity, to implement cavity QED with long cavities of low finesse [6–13]. A cavity is concentric when the cavity length l_{cav} matches twice the radius of curvature of the mirrors R_C. The mode function $u(\mathbf{x})$ (normalized to one at the field maximum) is tightly focused in the center of the cavity, leading to a small effective mode volume $V = \int d\mathbf{x}\, |u(\mathbf{x})|^2$ while the physical size of the cavity is large [11, 13]. In addition, the cavity decay rate $\kappa \propto 1/l_{\text{cav}}$ is reduced by the increased length of the cavity, which significantly eases the requirements for the mirror coatings. The resulting large coupling g_0 and low cavity decay rate κ make strong coupling between single atoms and single photons feasible even with low finesse cavities.

A second intriguing aspect of concentric cavities is that the frequencies of the higher-order transversal modes become degenerate. This could allow the realization of multimode cavity QED in the strong coupling regime [14].
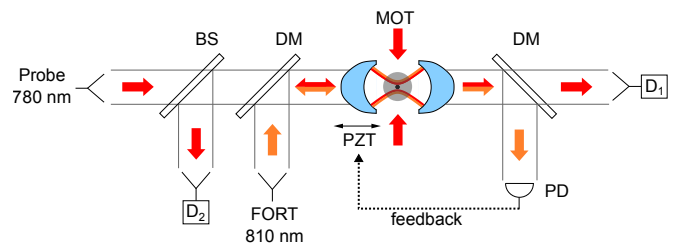

FIG. 1: Optical setup. A near resonant probe field at 780 nm impinges on the cavity to characterize the light-atom interaction. The transmitted and the reflected light is coupled into single mode fibers connected to avalanche photodetectors. The cavity length is stabilized close to the concentric length by a Pound-Drever-Hall lock to a frequency stabilized 810 nm laser. The intra-cavity field at 810 nm provides also a far-off-resonant standing-wave dipole trap for the atoms. BS: beam splitter with 70% reflectivity, DM: dichroic mirror, PZT: 3D-piezo actuator stack, PD: photodiode, MOT: magneto-optical trap, $D_{1(2)}$: avalanche photodetectors.

Different cavity modes could then effectively interact via a commonly coupled atom – constituting a novel platform for quantum information processing [15]. In this work we experimentally implement the idea of concentric cavity QED by trapping single ^{87}Rb atoms in a 11 mm long near-concentric cavity.

Cavity geometry. The cavity is composed of two nominally identical mirrors with a radius of curvature $R_C = 5.500(6)$ mm. To form a stable optical cavity, the stability parameter

$$g = 1 - l_{\text{cav}}/R_C \tag{1}$$

needs to satisfy $0 \leq g^2 \leq 1$ [16]. Thus, a concentric cavity with $l_{\text{cav}} = 2R_C$ is a limiting case at which the cavity is only marginally stable; the mode diameter at the position of the mirrors becomes infinite and the cavity highly susceptible to misalignment. However, we show that in practice the cavity can still be reliably operated extremely close to the concentric length.

We stabilize the cavity length by a Pound-Drever-Hall lock to a frequency-stabilized laser at a wavelength of

810 nm (Fig. 1) [17]. To accurately determine the cavity length l_{cav}, we analyze the frequency spacing of the transverse cavity modes by tuning the frequency of a probe field with a wavelength around 780 nm. We find a frequency spacing $\Delta\nu_{trans} = 109(2)$ MHz between the fundamental and first adjacent transverse mode. For a near-concentric cavity $\Delta\nu_{trans}$ is related to the cavity length via

$$\Delta\nu_{trans} = \frac{c}{2l_{cav}}\left(1 - \frac{\cos^{-1} g}{\pi}\right), \qquad (2)$$

where c is the speed of light [16]. The measured mode spacing indicates a cavity length $l_{cav} = 2R_C - 1.7(1)\,\mu m$, and a cavity parameter $g = -0.99969(2)$. At this length, the beam waist of cavity mode is expected to be $w_0 = \sqrt{\lambda l_{cav}/(2\pi)}\,[(1+g)/(1-g)]^{1/4} = 4.1\,\mu m$ [16]. *Cavity finesse and losses.* We further characterize the cavity by the transmission and reflection of the 780 nm probe field (Fig. 1). To achieve good mode matching between the fundamental mode of the cavity and the external probe field with Gaussian profile, we implement a so-called anaclastic lens design [18, 19]: The non-reflective back end of the mirrors have an ellipsoidal shape to act as an aspheric surface, converting the plane wavefront of a collimated Gaussian input beam to a converging spherical wavefront [13].

Varying the detuning $\Delta_c = \omega - \omega_c$ of the probe laser ω with respect to the cavity frequency ω_c, we record the reflection and transmission spectrum, which we fit to Lorentzian profiles. We obtain a full-width-at-half-maximum (FWHM) of 95(3) MHz and 99(1) MHz, respectively (Fig. 2a-b). Conservatively, we attribute the transmission linewidth to the fundamental mode of the cavity, $2\kappa = 2\pi \times 99(1)$ MHz, corresponding to a cavity finesse $F = \pi c/(2\kappa l_{cav}) = 138(2)$ [16]. Originally, the finesse of the cavity was higher $F \geq 500$ but dropped after bake-out of the vacuum chamber and operating the Rubidium dispenser. From the finesse and the nominal transmission $T = 0.5\%$ of the mirrors, we deduce a round-trip absorption loss L, the maximum in-coupling efficiency η, and resonant transmission T_{max} in the usual way [20] via

$$L = 2\pi/F - 2T = 3.6(1)\%, \qquad (3)$$
$$\eta = 1 - L^2/(2T + L)^2 = 39(1)\%, \qquad (4)$$
$$T_{max} = 4T^2/(2T + L) = 4.7(2)\%. \qquad (5)$$

In a direct measurement, we observe a cavity in-coupling efficiency of $\eta = 41.7(5)\%$, which agrees with Eq. 4 and demonstrates that the anaclastic design provides excellent mode matching between the probe field and the fundamental cavity mode (Fig. 2a). The resonant transmission $T_{max} = 4.6(2)\%$, measured directly after the cavity, is also in good agreement with Eq. 5. The transmission shown in Fig. 2b is lower because the transmitted light is coupled into a single mode fiber before detection.

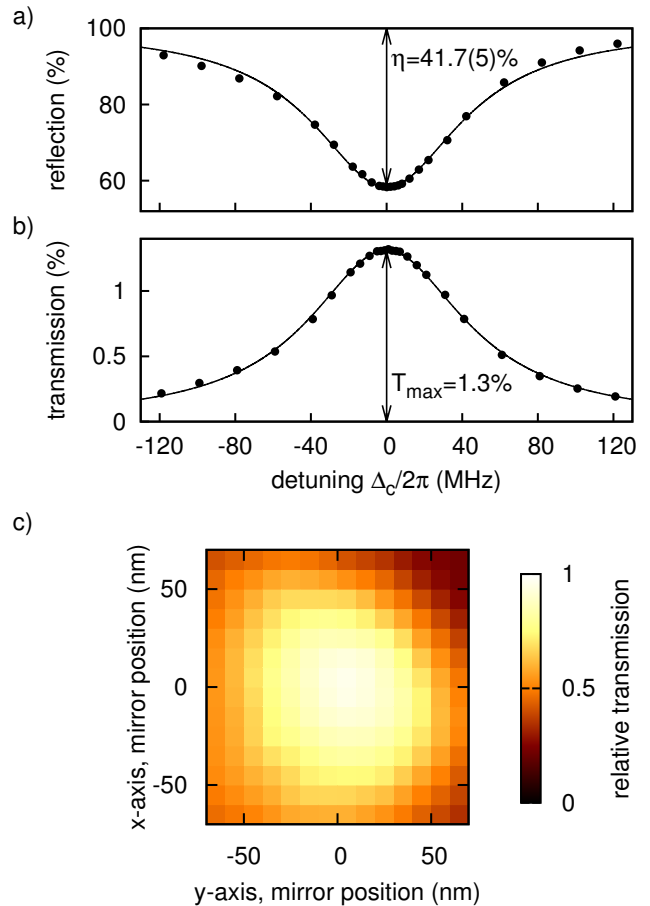*Cavity stability.* Approaching the concentric length $l_{cav} \to 2R_C$, the cavity becomes only marginally

FIG. 2: Tuning the frequency of the probe field with respect to the cavity resonance, we detect a) the reflection and b) the transmission spectrum after mode cleaning with the single-mode fiber. Solid lines are Lorentzian fits. c) Normalized cavity transmission as one mirror is transversally displaced. Throughout the experiment, the cavity length is actively stabilized to be resonant with the probe field.

stable, and consequently is highly sensitive to small misalignments. Therefore, one of cavity mirrors is placed on a 3D-piezo actuator stack which allows us to move the mirror 5 μm in each direction. Figure 2c shows the resonant transmission of the 780 nm probe field as we tune the transversal position of one mirror; the transmission shows a FWHM of 59(3) nm along both transverse directions. This high sensitivity to the transversal alignment requires active stabilization to compensate drifts caused, for example, by temperature fluctuations. Every 15 minutes an automatized alignment algorithm optimizes the transversal mirror position using the transmission of the 780 nm and 810 nm light as feedback signals; this procedure takes between 1-10 seconds and thus does not significantly reduce the experimental duty cycle.

Determining the atom-cavity interaction. To probe the light-atom interaction, we prepare a cold ensemble of ^{87}Rb atoms in a magneto-optical trap (MOT). The large physical separation of the two mirrors allows us
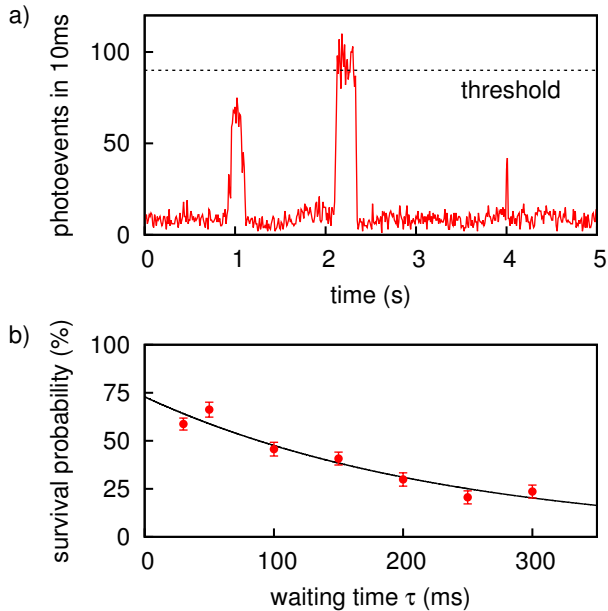
FIG. 3: a) Typical trace of detection events at detector D_1 with an atomic cloud in the MOT inside the cavity. The cooling light is 10 MHz red-detuned from the natural $5S_{1/2}$, $F=2$ to $5P_{3/2}$, $F=3$ transition frequency. The sudden increase of fluorescence indicates the entering of an atom into the FORT. At 1 s an atom is loaded into a side of the intra-cavity optical lattice which does not couple strongly to the cavity mode. We choose a high threshold value to select only strongly coupled atoms. b) Lifetime of single atoms in FORT without cooling light for a time τ. The solid line represents an exponential fit with a $1/e$-lifetime $t_0 = 230(30)$ ms.

to form the MOT inside the cavity. Atoms from the MOT are probabilistically loaded into the far off-resonant dipole trap (FORT) created by the intra-cavity field of the 810 nm light used to stabilize the cavity length. To account for the light shift induced by the FORT, the cavity length is set so that the resonance frequency is 22 MHz higher than the $5S_{1/2}$, $F=2$ to $5P_{3/2}$, $F=3$ transition. While operating the MOT, we detect the coupling of individual atoms to the fundamental cavity mode by the sudden increase of fluorescence at detector D_1 [21–23]. By choosing a high threshold value, we select atoms which couple strongly to the cavity mode. Figure 3 shows a typical fluorescent trace during the loading process, exhibiting a telegraph signal characteristic for single atom loading. The average duration between loadings events is typically 3-4 seconds. Thus, the low loading rate makes the simultaneous loading of two atoms in the center region of the cavity negligible. The lifetime of an atom in the trap is determined by switching off the cooling beams after a loading event for different waiting times τ. The survival probability $p(\tau)$ decays exponentially with a characteristic $1/e$ lifetime of 230(30) ms determined from a fit (Fig. 3b).

The single atom–cavity coupling g_0 can be determined from the cavity transmission and reflection [24, 25]. For a
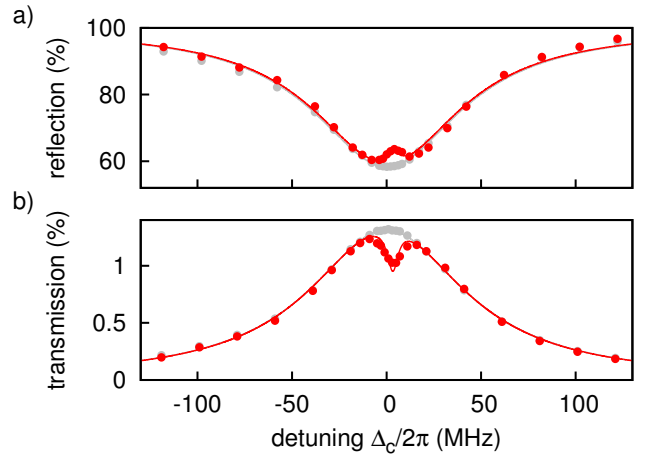
FIG. 4: Onset of the normal-mode splitting in the a) reflection and b) transmission spectrum when an atom is trapped in the FORT. Error bars are smaller than symbol size (one standard deviation). Red solid lines are fits based on Eq. 6. For comparison the empty cavity reflection/transmission (Fig. 2a) is shown in gray.

weak coherent beam, the coefficients for intensity transmission $T(\omega)$ and reflection $R(\omega)$ are given by

$$T(\omega) = \left| \frac{\kappa_T \left(i\Delta_a + \gamma \right)}{\left(i\Delta_c + \kappa \right)\left(i\Delta_a + \gamma \right) + g_0^2} \right|^2, \qquad (6)$$

$$R(\omega) = \left| 1 - \frac{2\kappa_T \left(i\Delta_a + \gamma \right)}{\left(i\Delta_c + \kappa \right)\left(i\Delta_a + \gamma \right) + g_0^2} \right|^2, \qquad (7)$$

with a cavity field decay rate through each mirror $\kappa_T = T\pi c/l_{\text{cav}}$, and the detuning $\Delta_a = \omega - \omega_a$ of the driving laser with respect to the atomic transition frequency ω_a [1]. Once an atom is loaded, we use an experimental sequence that alternates between 1 ms of probing the cavity transmission, and 1 ms of laser cooling by the MOT beams. The detected photoevents during the cooling cycle are used to check whether the atom is still present.

The atom-light interaction is revealed in the reflection– and transmission spectrum obtained by tuning the frequency of the probe laser. When an atom is present, the spectra show the onset of the normal-mode splitting (Fig. 4, red circles). From a least-squares fit of the transmission spectrum to Eq. 6 with two free parameters, we obtain an interaction strength $g_0 = 2\pi \times 5.0(2)$ MHz and a frequency offset $\omega_{\text{off}} = \omega_c - \omega_a = 2\pi \times 3.4(3)$ MHz between cavity and atomic resonance. The amplitude of the fit function $T(\omega)$ is set to the independently determined maximum transmission of the empty cavity. From g_0, the cavity linewidth $2\kappa = 2\pi \times 99(1)$ MHz, and the natural transition linewidth $2\gamma = 2\pi \times 6.07$ MHz, we obtain the single atom cooperativity $C_0 = g_0^2/(2\kappa\gamma) = 0.084(4)$.

The reflection spectrum is analyzed in a similar way by fitting to Eq. 7. For this, we use three fit parameters, $g_0 = 2\pi \times 4.6(4)$ MHz, the frequency offset $\omega_{\text{off}} = 2\pi \times 4.4(7)$ MHz, and the reflected power far away from

the atom/cavity resonance. The fits of Eq. 6-7 to the transmission and reflection reproduce the observed values very well (Fig. 4, solid lines), and lead to similar values for the atom-cavity coupling constant g_0 and the frequency offset ω_{off}.

The experimentally obtained value for g_0 is lower than expected for a two-level atom from the cavity geometry $g_0 = \sqrt{3\lambda^2 c\gamma/(4\pi V)} = 2\pi \times 12.1\,\text{MHz}$ where $V = \frac{\pi}{4}w_0^2 l_{\text{cav}} = 3 \times 10^5 \lambda^3$ is the effective mode volume in paraxial approximation [1]. We attribute this partly to the fact that in this experiment, the atom is prepared by the MOT beams in a random spin state m_F of the $5S_{1/2}$, F=2 manifold before the transmission is probed with a linearly polarized probe field. Averaging over the corresponding Clebsch-Gordan coefficients, we estimate that the atom-cavity coupling should be a factor $\sqrt{2}$ larger for a circularly polarized probe field driving an atom prepared in the $5S_{1/2}$, F=2, m_F=2 on a transition to the $5P_{3/2}$, F=3, m_F=3 state.

Discussion and conclusion. Our experiment demonstrates the prospects and challenges of concentric cavity QED. The realization of atom-cavity coupling exceeding the natural dipole decay rate by a factor $g_0/\gamma = 1.7(1)$ could stimulate further efforts employing concentric cavities. The coupling observed in this proof-of-principle experiment is already similar to many state-of-the-art experiments in the strong coupling regime, but with a cavity two orders of magnitude shorter [1]. Only in very short (few tens of μm long) cavities, significantly larger values of g_0/γ have been demonstrated [26, 27]. Going closer to the concentric length $l_{\text{cav}} \to 2R_C$ should increase the interaction strength even further. We estimate that a ratio $g_0/\gamma \geq 4$ can be achieved for $l_{\text{cav}} \approx 2R_C - 100\,\text{nm}$. When stabilizing the cavity near this point, we currently observe that the cavity finesse and transmission drop, possibly due to deviations of the mirror from an ideal spherical surface, and stronger coupling of the probe field to other higher-order transversal cavity modes.

Even without operating closer to the concentric length, we expect that a single atom cooperativity above unity can be reached by modestly increasing the finesse to $F = 1000$ and performing the probing on a cyclic transition. A medium cavity finesse of $F \geq 4500$ would put this system into the single atom-single photon strong coupling regime. We note that although we operate the cavity only $1.7(1)\,\mu$m shorter than the critical length, the expected intracavity diffraction losses are negligibly low as the mode radius on the mirror is an order of magnitude smaller than the aperture of the mirror [13]. While our experiments are performed with single neutral atoms, concentric cavities are also interesting for other quantum systems: examples are trapped ions [28] and Rydberg atoms [29, 30], which both are experimentally difficult to hold within short cavities due to the electric field noise near dielectric mirrors.

Acknowledgments

[1] A. Reiserer and G. Rempe, Rev. Mod. Phys. **87**, 1379 (2015).

[2] H. J. Kimble, Nature **453**, 1023 (2008).

[3] S. Ritter, C. Nolleke, C. Hahn, A. Reiserer, A. Neuzner, M. Uphoff, M. Mucke, E. Figueroa, J. Bochmann, and G. Rempe, Nature **484**, 195 (2012).

[4] J. G. Bohnet, K. C. Cox, M. A. Norcia, J. M. Weiner, Z. Chen, and J. K. Thompson, Nat Photon **8**, 731 (2014).

[5] O. Hosten, N. J. Engelsen, R. Krishnakumar, and M. A. Kasevich, Nature **529**, 505 (2016).

[6] S. E. Morin, C. C. Yu, and T. W. Mossberg, Phys. Rev. Lett. **73**, 1489 (1994).

[7] J.-M. Daul and P. Grangier, The European Physical Journal D - Atomic, Molecular, Optical and Plasma Physics **32**, 195 (2005).

[8] A. Haase, B. Hessmo, and J. Schmiedmayer, Opt. Lett. **31**, 268 (2006).

[9] C. Russo, H. G. Barros, A. Stute, F. Dubin, E. S. Phillips, T. Monz, T. E. Northup, C. Becher, T. Salzburger, H. Ritsch, P. O. Schmidt, and R. Blatt, Applied Physics B **95**, 205 (2009).

[10] F. Dubin, C. Russo, H. G. Barros, A. Stute, C. Becher, P. O. Schmidt, and R. Blatt, Nat Phys **6**, 350 (2010).

[11] S. A. Aljunid, B. Chng, J. Lee, M. Paesold, G. Maslennikov, and C. Kurtsiefer, Journal of Modern Optics **58**, 299 (2011).

[12] Y.-J. Chen, S. Zigo, and G. Raithel, Phys. Rev. A **89**, 063409 (2014).

[13] K. Durak, C. H. Nguyen, V. Leong, S. Straupe, and C. Kurtsiefer, New Journal of Physics **16**, 103002 (2014).

[14] A. Wickenbrock, M. Hemmerling, G. R. M. Robb, C. Emary, and F. Renzoni, Phys. Rev. A **87**, 043817 (2013).

[15] M. L. Terraciano, R. Olson Knell, D. G. Norris, J. Jing, A. Fernandez, and L. A. Orozco, Nat Phys **5**, 480 (2009).

[16] B. E. A. Saleh and M. C. Teich, "Resonator optics," in *Fundamentals of Photonics* (John Wiley & Sons, Inc., 2001) pp. 310–341.

[17] R. W. P. Drever, J. L. Hall, F. V. Kowalski, J. Hough, G. M. Ford, A. J. Munley, and H. Ward, Applied Physics B **31**, 97 (1983).

[18] I. Sahl, "On burning mirrors and lenses (publisher unknown, baghdad, 984), (see the next reference also)," (984).

[19] R. Rashed, Isis **81**, pp. 464 (1990).

[20] C. J. Hood, H. J. Kimble, and J. Ye, Phys. Rev. A **64**, 033804 (2001).

[21] H. Mabuchi, Q. A. Turchette, M. S. Chapman, and H. J.

Kimble, Opt. Lett. **21**, 1393 (1996).

[22] C. J. Hood, M. S. Chapman, T. W. Lynn, and H. J. Kimble, Phys. Rev. Lett. **80**, 4157 (1998).

[23] J. Ye, D. W. Vernooy, and H. J. Kimble, Phys. Rev. Lett. **83**, 4987 (1999).

[24] M. G. Raizen, R. J. Thompson, R. J. Brecha, H. J. Kimble, and H. J. Carmichael, Phys. Rev. Lett. **63**, 240 (1989).

[25] R. J. Thompson, G. Rempe, and H. J. Kimble, Phys. Rev. Lett. **68**, 1132 (1992).

[26] C. J. Hood, T. W. Lynn, A. C. Doherty, A. S. Parkins, and H. J. Kimble, Science **287**, 1447 (2000).

[27] R. Gehr, J. Volz, G. Dubois, T. Steinmetz, Y. Colombe, B. L. Lev, R. Long, J. Estève, and J. Reichel, Phys. Rev. Lett. **104**, 203602 (2010).

[28] M. Brownnutt, M. Kumph, P. Rabl, and R. Blatt, Rev. Mod. Phys. **87**, 1419 (2015).

[29] A. Tauschinsky, R. M. T. Thijssen, S. Whitlock, H. B. vanLindenvandenHeuvell, and R. J. C. Spreeuw, Phys. Rev. A **81**, 063411 (2010).

[30] R. P. Abel, C. Carr, U. Krohn, and C. S. Adams, Phys. Rev. A **84**, 023408 (2011).